[1] Dongyang Chen,
[2]Xiangyong Tan,
[3]Jiaye Lin
[4,*]E Xia

A remote sensing image object detection algorithm based on transfer learning

Journal of Electrical Systems

Abstract: - As a method to obtain and process remote sensing images by using remote sensing technology, remote sensing image analysis has been extensively used in various important fields. It plays a key role in environmental monitoring, resource management, urban planning, agricultural forestry, disaster monitoring, climate research, military reconnaissance, public safety, transportation, biomedicine, etc. To solve the problems of remote sensing images such as variable object scale, fuzzy object, and complex background, a remote sensing small sample object detection algorithm RE-FSOD based on feature reweighting was proposed.The model consists of a meta-feature extractor, a feature reweighting extractor, and a prediction module. The meta-feature extractor is composed of CSPDarknet-53, FPN and PAN, and it is responsible for extracting the meta-features of the data; The feature reweighting extractor is used to generate feature reweighting vectors, which are used to adjust meta-features to strengthen features that help detect new categories; The prediction module is composed of the prediction module of YOLOv3.On this basis, the positioning loss function is replaced by the CIOU loss function to improve the positioning accuracy of the model.Finally, training and testing were carried out on the NWPUVHR-10 remote sensing data set. The experimental results revealed that compared with the baseline method FSODM, the method was improved by about 19 %, 11 % and 8 % in the case of 3-shot, 5-shot and 10-shot, respectively.

Keywords: Small sample object detection; YOLO; Transfer learning; Feature reweighting; Attention mechanism.

I. INTRODUCTION

Remote sensing images are characterized by large object scale differences, fuzzy objects, and high background complexity. The above small sample object detection algorithms are mostly developed based on common objects in daily life, and the accuracy of object detection tasks in remote sensing images is still low. Most are based on the two-stage FasterRCNN algorithm, with high computational complexity and slow detection speed.Based on the one-stage YOLOv3, FSODM proposed a multi-scale feature reweighted extractor for remote sensing images, which improved the detection accuracy of objects at different scales and had a faster detection speed. However, the deep semantic and shallow positioning information of the images extracted by FSODM are still not rich enough. To solve the above problems, a new feature reweighting small sample object detection algorithm (RE-FSOD) was proposed based on FSODM.

Object detection aims to find the objects in images or videosthat people are interested in and detect their location and size simultaneously. Object detection not only solves the categoryification problem but also solves the positioning problem. As one of the basic problems of computer vision, object detection constitutes the basis of many other visual tasks, such as instance segmentation, image annotation, and object tracking.The object detection algorithm can be divided into a one-stage object detection algorithm and a two-stage object detection algorithm. The former mainly includes YOLO[1-3], SSD[4] and other algorithms; the latter mainly includes RCNN[5], FastRCNN[6], FasterRCNN[7], and so on. The one-stage object detection algorithm reduces the occupation of space and time, and the speed is greatly improved, but its accuracy is lower than the two-stage object detection algorithm. The performance of the above algorithms depends on a large number of data sets, but in some scenarios, it is often difficult to collect a large number of data sets or it is quite expensive to obtain data sets[8].

II. RE-FSOD ALGORITHM

A. Small sample object detection problem setting

The small sample object detection algorithm aims to learn the general meta-knowledge from the source data set D_i, and uses a small number of target data sets D_o to transfer the meta-knowledge to the target task, so that the small sample object detection algorithm can quickly converge on the target data set. It was assumed that there

[1]School of automation, Central South University, Changsha,410083, Hunan,China
[2]School of automation，Central South University, Changsha,410083, Hunan,China
[3]The College of Mechanical and Electrical Engineering, Central South University,Changsha,410083, Hunan,China
[4,*] Correspondingauthor: School of automation, Central South University,Changsha,410083, Hunan,China

were N types of samples in the target data set, and each type had K labels, which was called the N-way-K-shot task[20].

The data set of the small sample target detection algorithm consists of a support set and a query set. Given a k-shot task, the support set is $S_i = \{(I_k, M_k)\}$, where I_k represents the input image and $I_k \in R^{h\times w\times 3}$; M_k represents the mask of the corresponding target, and $k = 1,2,3,\cdots,K$. The query set Q_i contains N_q pictures, and N_q is the number of all pictures in the training set or the test set and also contains k types of objects. The input of an iterative training of the RE-FOSD algorithm is $T_i = \{Q_i, S_i\}$.

B. Introduction to FSODM

The FSODM algorithm is the first small sampleremote sensing object detection algorithm proposed by Li et al.in 2021. It was developed based on the YOLOv3 object detection algorithm. On this basis, a multi-scale feature reweighting module was introduced to adjust the features of the feature map and strengthen those features that help detect new types so that the algorithm can achieve better detection accuracy under a small number of samples.Compared with other popular small sample object detection algorithms such as TFA and FSCE, FSODM combines a multi-scale feature reweighting module to better deal with remote sensing targets with variable scales[9]. The FSODM algorithm was developed based on the one-stage YOLOv3 algorithm. The new feature reweighting module can be removed in the inference stage, with less computation and faster inference speed. However, the detection accuracy of the FSODM is still low. Therefore, to identify remote sensing targets more accurately, the algorithm still needs to be further improved. The structure of the FSODM is shown in Figure 1.

C. Overall structure of RE-FSOD

The RE-FSOD algorithm is based on the FSODM and has the same architecture as the FSODM. It is also composed of a meta-feature extractor, a feature reweighting extractor, and a prediction module[10-11]. The overall architecture is shown in Figure 2, and the detailed structure is shown in Figure 3.

The input of the meta-feature extractor is the pictures in the query set, and it can extract three meta-feature maps with different scales. The feature reweighting extractor generates three scale-specific category feature reweighting vectors for all target categories in the data set. 1×1channel convolution is conducted on the feature reweighting vector of the corresponding scale and the meta-feature map to adjust the weight of the meta-feature map, strengthen the features that help detect new types, and input the feature map into the prediction module to generate (x, y, w, h, o, c) , where (x, y, w, h) represents the bounding box coordinates, o represents the confidence, and c represents the category score..

III. KEY TECHNOLOGIES OF RE-FOSD

A. Meta-feature extractor

The meta-feature extractor aims to extract robust meta-features from the query set. I is the query image input to the meta-feature extractor, and $I \in R^{h\times w\times c}$. The extracted meta-features are $F_i = \varepsilon(I) \in R^{h_i\times w_i\times m_i}$, where i represents the serial number of the three scales ($i = 1,2,3$), and h_i, w_i, m_i represent the size of the feature map of scale i. According to the setting of the FSODM, the image input of the feature extractor is set to 512×512, and the sizes of the three feature maps are $16\times 16\times 1024$,$32\times 32\times 512$, and $64\times 64\times 256$, respectively.

The meta-feature extractor in FSODM is composed of a Darknet-53 and a feature pyramid network (FPN). The RE-FSOD replaced the backbone network of the meta-feature extractor with CSPDarknet-53, and the PAN structure was added based on the FPN. There were a large number of residual blocks in Darknet-53, and the convolution layer Conv2D with a step size of 2 and a convolution kernel size of 3×3 was used toreplace the pooling layer for downsampling. The residual block could increase the depth of the network so that the network could extract more advanced semantic features and avoid the disappearance or explosion of the gradient.Compared with the Darknet-53 network, the CSPDarknet-53 introduceda CSP structure in the residual structure. CSP divided the original input into two branches, used 1×1 convolution for feature transformation, and halved the number of channels in the feature map. The feature map of one branch passed through N

BottleNeck modules and finally connected on the channel dimension. The structure of CSP shunt can reduce the amount of calculation and effectively transmit information so that the network can better learn features.

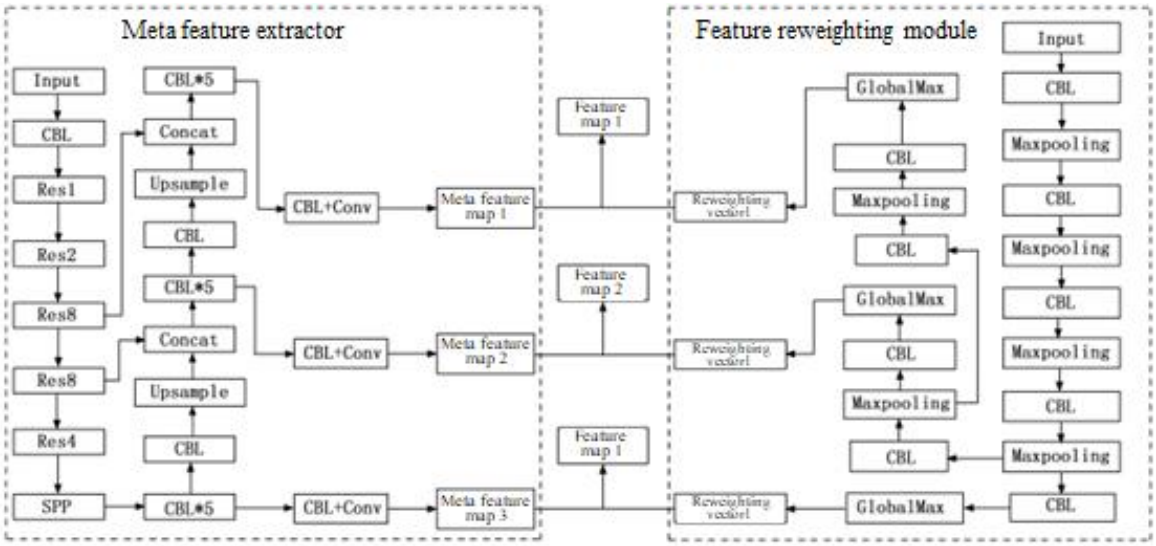

Figure1 Network structure of FSODM

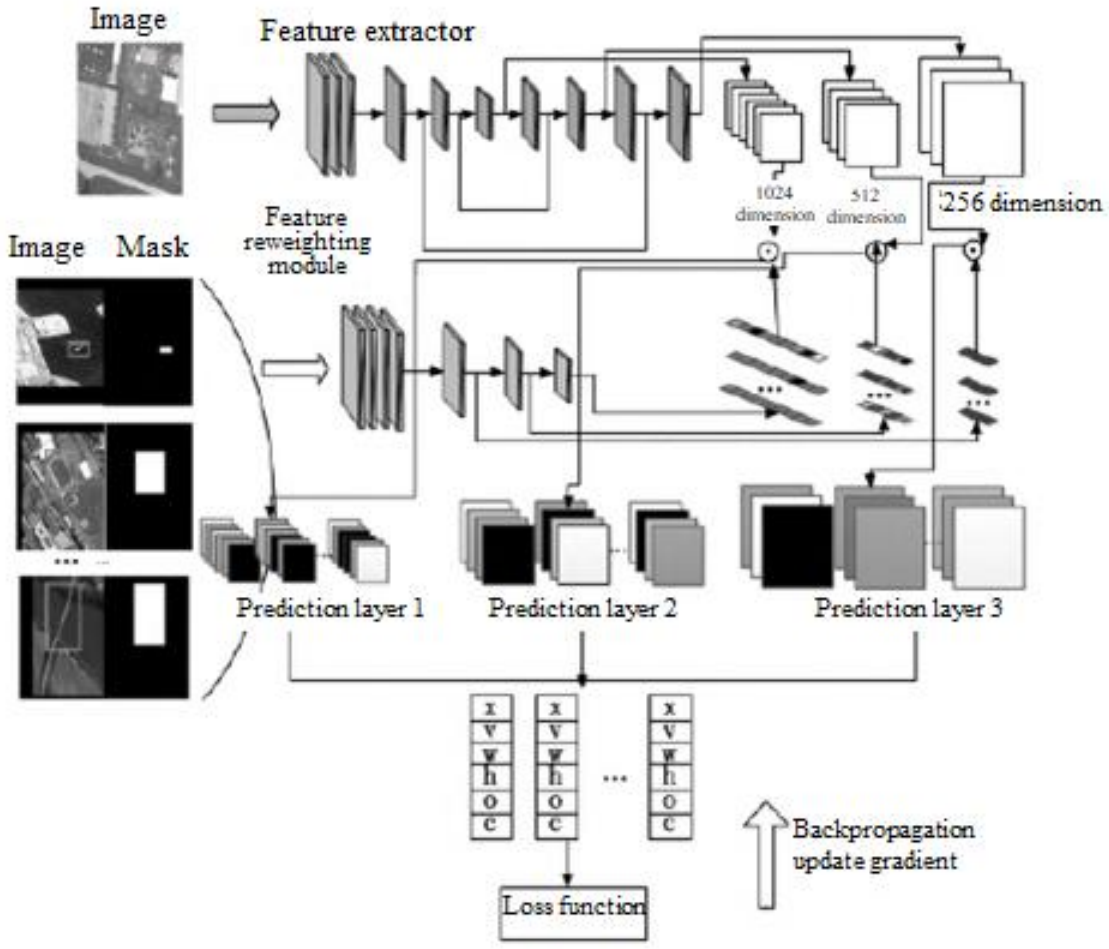

Figure 2 Architecture of RE-FSOD structure

The CSPDarknet-53 used the SPPF (Maximum Pooled Feature Pyramid) module. In the original method, the method used in the backbone network is SPP. Both aims to fuse local features and global features. There are four branches in the SPP, one of which is the convolution layer, and the other three branches are the maximum pooling layers with convolution kernels of 5,9,13, and then the output of the four branches is connected in the channel dimension. The local and global features are fused to extract the target features with different sizes. SPPF has been improved on the SPP structure and the existing feature maps were reused. Besides, the convolution kernel of the three maximum pooling layers was set to 5, greatly improving the inference speed.

Generally, the shallow feature map has more positioning information and less semantic information, and the deep feature map becomes smaller in size and larger in dimension. Therefore, the deep feature map has more semantic information and less positioning information. The FPN structure was used in the FSODM meta-feature extractor. FPN is a top-down feature pyramid, which passes down the shallow semantic features and enhances the entire pyramid. Meanwhile, it only enhances the semantic information but does not pass the positioning information. Aiming at the shortcomings of FPN, the PAN structure added a bottom-up pyramid based on the FPN to supplement FPN and pass the positioning features up. The generated feature map had rich positioning and semantic information simultaneously, thus improving the accuracy of the object detection algorithm.

B. Feature reweighting extractor

The input of the feature reweighting extractor is the region of interest (ROI) of the detected object, as shown in Figure 1.It contains the pictures of each category and the mask of the corresponding categoryobject. Generally, the input image contains multiple detection objects. To make the feature reweighting extract able to identify the object of a specific category, only one object of the corresponding categorywas selected. According to this object position, the region pixels in the bounding box were set to 1 and the pixels in the remaining positions were set to 0 to obtain the mask. The input image and the mask were spliced into a 4-dimensional vector and input into the feature reweighting extractor to generate a feature reweighting vector corresponding to multiple scales of the category. The feature reweighting vector and the meta-feature map were convoluted by 1×1 to adjust the meta-feature map and strengthen the features that help detect new categoryes.

In FSODM, the convolution layer and the maximum pooling layer were used to form a feature reweighting network. A C2fSE module with an attention mechanism was proposed to make the feature reweighting extract richer semantic information. On this basis, the C2fSE module was integrated into the feature reweighting extractor. The C2fSE module is composed of a C2f module and a SE module. The convolution layer of the C2f module expands the receptive field by increasing the size and stride of the convolution kernel so that the model can obtain features in a larger area. At the same time, the residual structure in C2f can deepen the number of layers of the network and enhance the feature extraction ability of the network.The Squeeze-and-Excitation (SE) attention mechanism first compresses the two-dimensional features of each channel into a real number through a compression operation to obtain the global features of the channel dimension and then generates a weight for each channel through an incentive operation. Finally, the obtained weight is used to adjust the initial feature map. The SE makes the model pay more attention to the features with a large amount of information through the operation of extrusion and excitation, thereby suppressing those unimportant features and improving the feature extraction ability of the feature reweighting network.

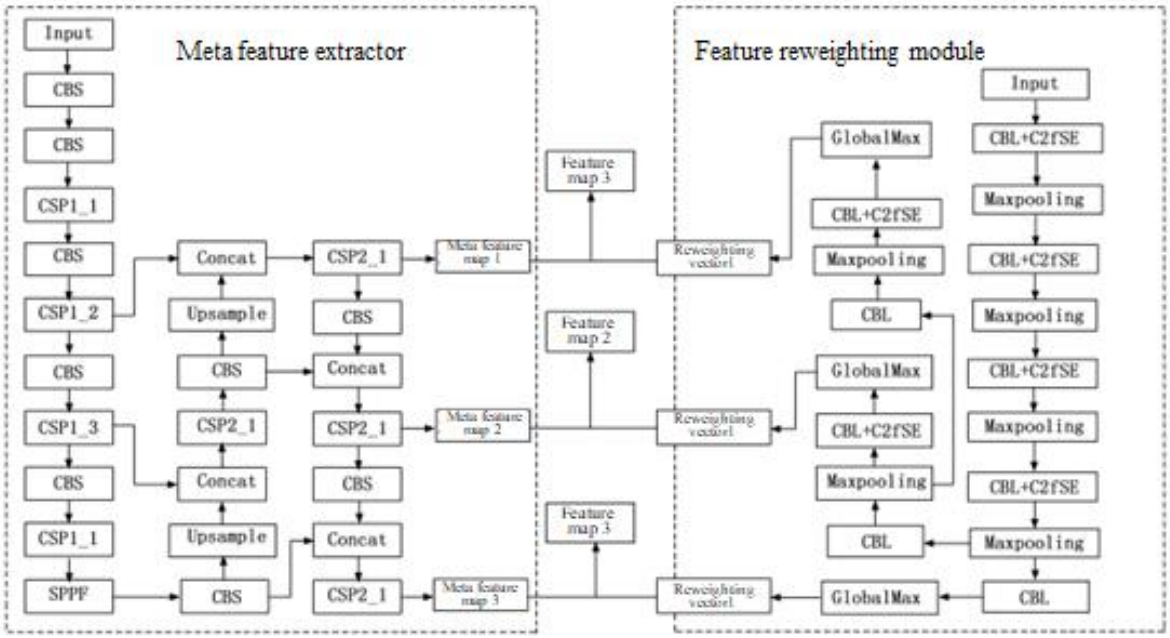

Figure 3 Network structure of RE-FSOD

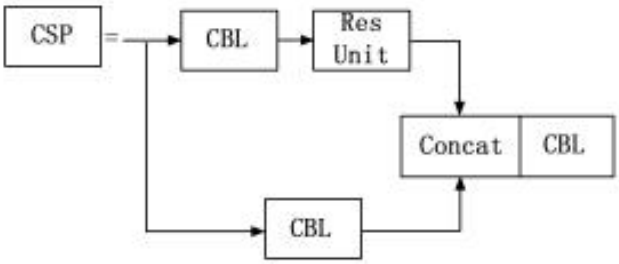

Figure 4 Structure of CSP

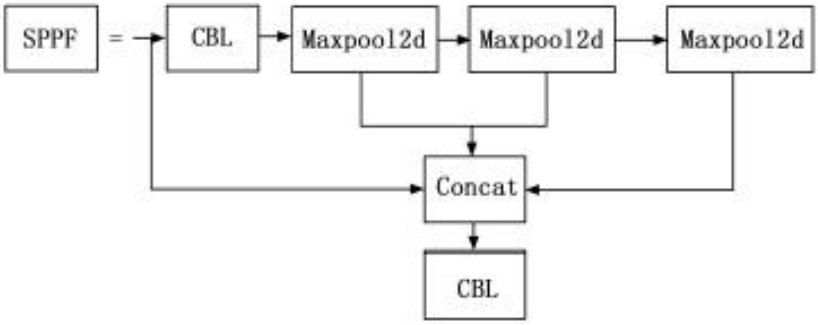

Figure 5 Structure of SPP

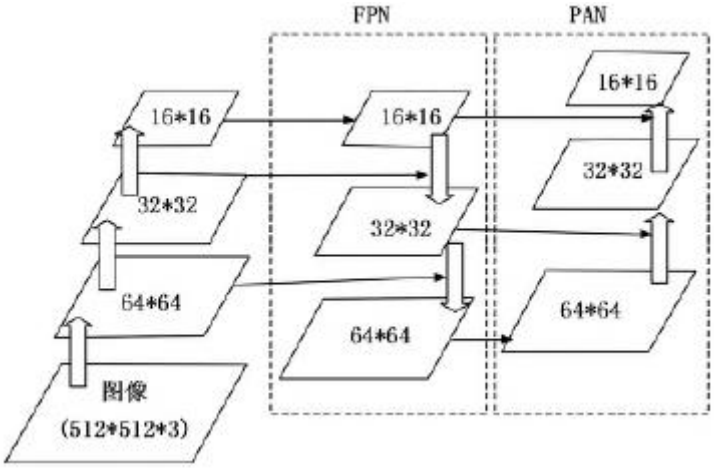

Figure 6 Structure of 6FPN+PAN

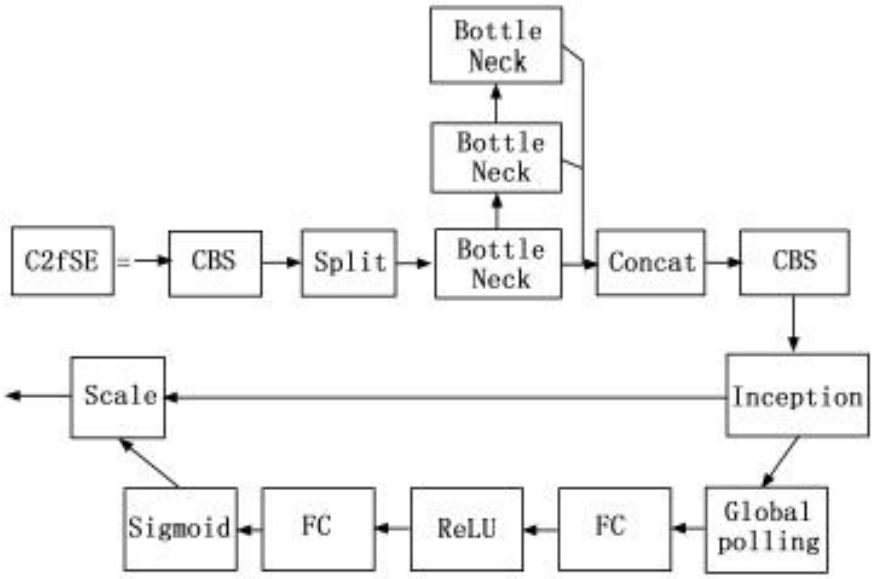

Figure 7 Structure of C2fSE

C. Loss function

The FSODM loss function consists of positioning loss, category loss, and confidence loss. Compared with FSODM, the RE-FSOD replaced the positioning loss from mean square error loss to CIOU loss.

The mean square error loss formula of the FSODM is shown in Equation (1) :

$$L_{\text{loc}} = \frac{1}{N_{\text{pos}}} \sum_{\text{pos}} \sum_{l} \left(\text{coord}_t^l - \text{coord}_p^l \right)^2 \quad (1)$$

Where $l \in \{x, y, w, h\}$, xand y are the center points of the bounding box, w and h are the width and height of the prediction box, respectively. If the IOU between the anchor and the real box is greater than 0.5 or the anchor has the largest IOU in all anchors and a real box, the anchor is considered as a positive sample, otherwise, the anchor is considered as a negative sample. pos represents all positive samples, coord_t^l is the predicted bounding box, and coord_p^l is the real box.When large objects has the same IOU as the small objects. According to the formula of mean square error, the loss of large objects must be greater than that of small ones, resulting in inconsistent loss of target location at different scales. Therefore, the loss function was replaced by the CIOU loss function. The CIOU loss function took IOU as the loss value, which unified the losses of different scale targets. Meanwhile, the CIOU loss function took into account the distance between the prediction box and the center point of the real box and the aspect ratio between the prediction box and the real box, accelerating the convergence of the model and improving the positioning accuracy of the model. IOU is the degree of overlap between the prediction box and the real box, and its calculation formula is shown in (2):

$$\text{IOU} = \frac{A \cap B}{A \cup B} \quad (2)$$

Where A represents the area of the prediction box, and B represents the area of the real box.

The aspect ratio penalty term of the CIOU loss function is shown in Equation (3):

$$V = \frac{4}{\pi^2} \left(\arctan \frac{w^{gt}}{h^g t} - \arctan \frac{w}{h} \right)^2 \quad (3)$$

Where w_{gt} and h_{gt} are the width and height of the real box, and w and h are the width and height of the prediction box.

The CIOU center pointdistance penalty term was defined by Equations (4) and (5):

$$D = \frac{d}{c^2} \quad (4)$$

$$d = \rho^2 \left(A_{\text{ctr}}, B_{\text{ctr}} \right) \quad (5)$$

Where A_{ctr} and B_{ctr} represent the center points of the real box and the prediction box; $\rho^2(\bullet)$ represents the Euclidean distance between the two points; c represents the diagonal of the maximum circumscribed rectangle of the real box A and the prediction box B; and d represents the distance between the center points of A and B.

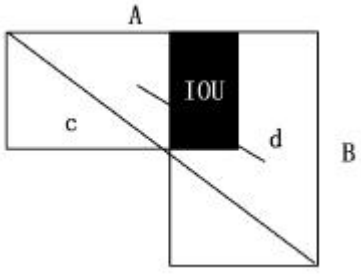

Figure 8 Center point distance

Where α is the weight coefficient, as shown in Equation (6) :

$$\alpha = \frac{V}{(1 - IOU) + V} \quad (6)$$

The final definition of the CIOU loss function is shown in Equation (7) :

$$L_{\text{ciou}} = 1 - \text{IOU}\left(A, B\right) + \frac{\rho^2\left(A_{ctr}, B_{ctr}\right)}{c^2} + \alpha V \quad (7)$$

The confidence loss of positive samples is shown in Equation (8) :

$$L_{\text{obj}} = \frac{1}{N_{\text{pos}}} \sum_{\text{pos}} -\left[P_t \cdot \log P_{\text{o}} + \left(1 - P_t\right) \cdot \log\left(1 - P_o\right)\right] \quad (8)$$

Where p_0 represents the predicted confidence coefficient, and o represents the possibility of the existence of the object in the prediction box. p_t is the value of the real box, and it is 1 when there is an object, and 0 when there is no object.

The confidence loss of negative samples is shown in Equation (9) :

$$L_{\text{noobj}} = \frac{1}{N_{\text{neg}}} \sum_{\text{meg}} -\left[P_t \cdot \log P_o + \left(1 - P_t\right) \cdot \log\left(1 - P_o\right)\right] \quad (9)$$

Where neg represents all negative samples.

The total confidence loss is shown in Equation (10) :

$$L_0 = L_{\text{obj}} \cdot w_{\text{obj}} + L_{\text{nobj}} \cdot w_{\text{nobj}} \quad (10)$$

Where, w_{obj} and w_{nobj} are the weight of positive and negative sample losses, which are used to balance the positive and negative sample losses. The category loss is shown in Equation (11) :

$$L_c = \frac{1}{N_{\text{pos}}} \sum\nolimits_{\text{pos}} -\log\left(\frac{e^{c_{pt}}}{\sum_{i-1}^{N} e^{c_{pj}}}\right) \quad (11)$$

Where c_{pt} is the real category score, and c_{pj} is the predicted category score. The confidence has been used to determine whether there is an object in the prediction box, so the categoryification loss ignores the negative sample.

The total loss function of RE-FSOD is expressed as:

$$L = L_{\text{ciou}} + L_{\text{obj}} + L_c \quad (12)$$

D. Prediction module

The prediction module is similar to YOLOv3. According to the setting of YOLOv3, the method based on anchor (anchor frame) was adopted. The size of the anchor corresponding to large objects was set to (116×90), (156×198), and (373×326), the size of medium objects was set to (30×61), (62×45), and (59×119), and the size of small objects was set to (10×13), (16×30), and (33×23). The three-scale feature maps were input into the prediction module to generate $\left(x, y, w, h, o, c\right)$, where $\left(x, y, w, h\right)$ represents the bounding box coordinates, o represents the confidence and c represents the category score.Compared with the YOLOv3 prediction module, only category prediction was different. Each prediction box of YOLOv3 generated k category scores. As the RE-FSOD had a category feature map for each category, each prediction box only predicted a category score c. A set of prediction boxes corresponding to the same position of the input image was called $c_{pi}\left(I = 1, 2, \cdots, K\right)$, and the final probability of each prediction box category is:

$$P_{ci} = \frac{e^{c_{pi}}}{\sum_{j=1}^{K} e^{c_{pi}}} \quad (13)$$

Where $\sum_{j=1}^{K} P_{Ci} = 1$.

E. Training and reasoning processes

The data set used the public NWPUVHR-10 ten-category remote sensing data set, and selected ships, storage tanks, basketball courts, baseball courts, automobiles, ground tracks, and ports as the base categories, and aircraft, baseball courts, and tennis courts as new categories. The training strategy was based on the settings in the FSODM. The training process was divided into two stages: in the first stage, the training was carried out on the base category with sufficient labels, called base category training; in the second stage, the model generated in the first stage was used to fine-tune on the small sample data set.The data set D_{train} of basic training included 640 pictures of 7 categories of objects, including 240 ship objects, 524 tank objects, 127 basketball court objects, 130 ground track objects, 180 port objects, 99 bridge objects, and 472 automobile objects. Under the k-shot task, the small sample data set D_{test} in the fine-tuning phase included 10 categories of targets, and the pictures in the base category data set were randomly selected until the selected pictures contained k objects of all categories.According to the setting in 1.1, the input of each iteration was $T_i = \{Q_i, S_i\}$. A query image corresponds to a set of support images. The support image was composed of the image and the mask of the corresponding target category as shown in Figure 9. In one round of training, the query image was all the images of the training set, and the corresponding support image was generated by the random combination of the images in the training set.

The training and reasoning processesare as follows:

1) Generate the base class training set D_{train} and the small sample data set D_{test} for inference.

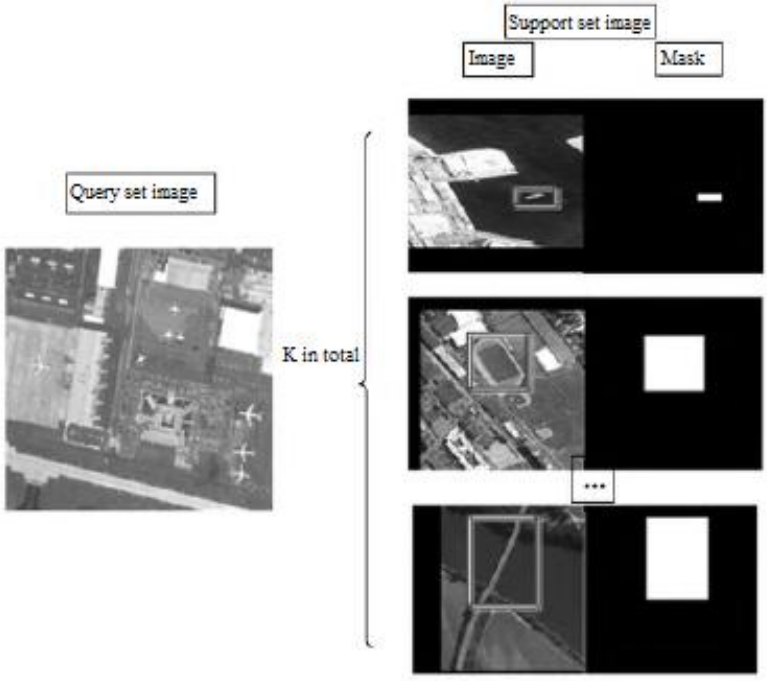

Figure 9 Schematic diagrams of query image and support image

2) Initialize the network weights of the feature extractor, the feature reweighting network and the prediction module.

3) Input the data in D_{train} into the network to train 900 rounds and save the model.

4) Load the model in Step 3), and use D_{test} to train 10 rounds for fine-tuning to generate the final model.

5) Use the data set in D_{test} , and input the support set into the feature reweighting network to generate the reweighting vector.

6) Input the query image into the network to generate the meta-feature map. Use the reweighting vector and the meta-feature map to carry out 1×1 channel convolution and generate the adjusted meta-feature map, which was input into the prediction module for decoding to generate the final prediction result. In the decoding process, only category prediction was different from YOLOv3, and the rest were the same.

IV. EXPERIMENT AND RESULT ANALYSIS

A. Experiment

To verify the performance of the RE-FSOD algorithm, it was compared with the current popular small sample object detection algorithms such as FSODM, TFA, FSCE, and PAMS-Det. The results are shown in Table 1. Compared with the PAMS-Det algorithm with the best performance, the mAP of the RE-FSOD improved by 14%, 10%, and 7% in the case of 3-shot, 5-shot, and 10-shot, respectively.

The RE-FSOD was improved based on the FSODM algorithm. To verify the performance of the improved RE-FSODmodule, the experiment shown in Figure 10 was carried out. In the 10-shot scene, the RE-FSOD could reduce the situation of misclassification and omission compared with the FSODM algorithm, which verified the superiority of the improved module.

B. Feature reweighting vector evaluation

To verify the effect of the feature reweighting module, as the high-dimensional vector was difficult to visualize, the T-SNE module was employed to reduce the dimension. In the T-SNE algorithm, the distribution of the high-dimensional vector was relatively close to that of the reduced-dimensional vector. However, if there was a distance in the high-dimensional vector, the distance of the reduced-dimensional vector would be widened. Intuitively, if the original distance in the high-dimensional space was very close, the distance after dimensionality reduction was still very close, but if there was a distance in the high-dimensional space, the distance after dimensionality reduction would be widened. This feature was conducive to the dimensionality reduction and visualization of the reweighting of 1024, 512, and 256-dimensionhigh-latitude features.

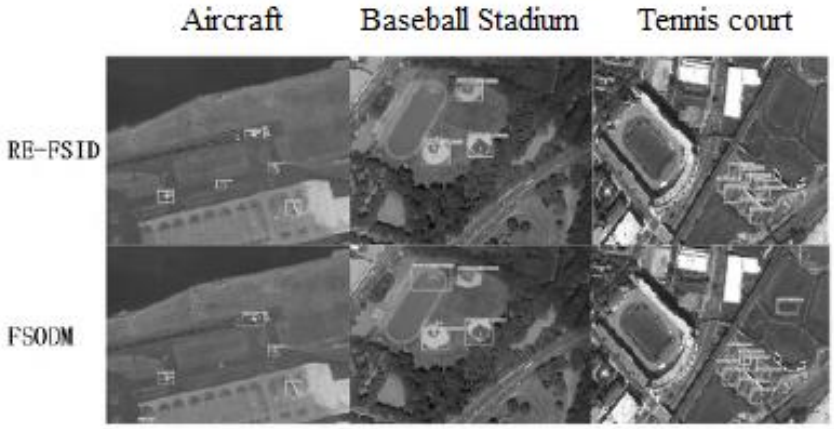

Figure 10 Comparison of experimental results

Table 1 Experimental results of different algorithms mAP50

Method	Sample size	Airplane	Baseball field	Tennis court	Average
FSODM	3	0.15	0.57	0.25	0.32
	5	0.58	0.84	0.16	0.53
	10	0.60	0.88	0.48	0.65
TFA	3	0.12	0.61	0.13	0.29
	5	0.51	0.78	0.19	0.49
	10	0.60	0.85	0.49	0.65
FSCE	3	0.37	0.52	0.24	0.40
	5	0.48	0.67	0.28	0.48
	10	0.57	0.83	0.37	0.59
PAMS-Det[21]	3	0.21	0.76	0.16	0.37
	5	0.55	0.88	0.20	0.55
	10	0.61	0.88	0.50	0.66
RE-FSOD	3	0.30	0.86	0.37	0.51
	5	0.63	0.87	0.46	0.65
	10	0.78	0.88	0.53	0.73

A total of 140 images were randomly selected from the support set of the base class training set and input into the feature reweighting module to generate reweighting vectors, with 20 images for each category. TSNE was used to reduce the high-dimensional data to 2D for visualization.

Different points represent different categories of feature reweighting vectors. It can be seen that the reweighting vectors of the same category were clustered together, which indicated that the reweighted module could successfully represent the category information from the original input image after gradient descent. The clustering effect was evaluated using the Euclidean distance from the sample point to the center point. The formula is as follows:

$$D=\sqrt{\left(x_1-x_{\text{mean}}\right)^2+\left(y_1+y_{\text{mean}}\right)^2} \quad (14)$$

Where $\left(x_{\text{mean}}, y_{\text{mean}}\right)$ represents the coordinate of the class center point and $\left(x_1, y_1\right)$ represents the coordinate of the sample point.

By calculating the average Euclidean distance between all sample points and their class center points, the average Euclidean distance of 256 dimensions was 785, the average Euclidean distance of 512 dimensions was 689, and the average Euclidean distance of 1024 dimensions was 627, indicating that the clustering result of 1024-dimension feature reweighting vector was better than that of 512-dimension and 256-dimension feature reweighting vectors. Therefore, the feature reweighting vector with higher dimensions carries more information and can better represent the category information in the support sample.

V. CONCLUSION

Based on the FSODM method, the RE-FSOD used CSPDarknet-53 as the backbone network in the meta-feature extractor, and PAN and SPPF structures were added, which could extract more robust meta-features. The C2fSE module combining attention mechanism and residual structure was introduced into the feature reweighting extractor, which could extract richer semantic information. Besides, CIOU was used as the positioning loss function to improve the positioning accuracy and accelerate the algorithm's convergence. The experiment showed that the higher the dimension of the specific reweighting vector, the richer the semantic information of the extracted specific category reweighting vector. Compared with the three improved methods proposed by FSODM, RE-FSDO could effectively improve the detection accuracy of the algorithm. Moreover, it hadmore obvious advantages than other advanced small sample target detection methods, indicating that the method can better deal with remote sensing images with variable scales, complex backgrounds, and blurred objects. Currently, the reasoning speed, calculation amount and memory occupation of the RE-FOSD still need to be further improved. In the future, the model will be lightweight by using methods such as pruning and quantization, which will reduce the parameters of the model and improve the reasoning speed of the model while ensuring the accuracy of the model.

REFERENCES

[1] Li Li, Peng Na, and Wang Wei "A Remote Sensing Image Detection Model Based on Lightweight Convolutional Neural Networks." Computer Engineering and Design 44.5 (2023): 1511-1518

[2] Li Shutao, Wu Qiong, Kang Xudong. Frontiers and Challenges of Intrinsic Information Decomposition in Hyperspectral Remote Sensing Images [J]. Journal of Surveying and Mapping, 2023, 52 (7): 1059-1073

[3] Zhou Yuan, Yang Qingqing, Ma Qiang, et al. Detection of tilted targets in first-order fully convolutional remote sensing images [J]. Chinese Journal of Image Graphics, 2022, 27 (8): 12

[4] Jin Ruijiao and others "Multi scale rotating object detection in optical remote sensing images based on DETR and improved denoising training." Laser and Optoelectronics Progress 61.2 (2024): 0211023

[5] Chadong Equality "Research on Rapid Reading and Display Method of Remote Sensing Image Data Based on GDAL." 1 (2022)

[6]Yu Z, Pei J, Zhu M, et al. Multi-attribute adaptive aggregation transformer for vehicle re-identification[J]. Information Processing & Management, 2022, 59(2): 102868.

[7] Han Min, Yang Xue. Improved Bayesian ARTMAP transfer learning remote sensing image classification algorithm [J]. Journal of Electronic Science, 2016, 44 (9): 6. DOI: 10.3969/j. issn.0372-2112.2016.09.033

[8]Jan N, Gwak J, Pei J, et al. Analysis of networks and digital systems by using the novel technique based on complex fuzzy soft information[J]. IEEE Transactions on Consumer Electronics, 2022, 69(2): 183-193.

[9] Lin Yu, Zhao Quanhua, Li Yu. A remote sensing image classification method based on deep transfer learning [J]. Journal of Earth Information Science, 2022, 24 (3): 13. DOI: 10.12082/dqxxkx.2022.210428
[10]Zhong K, Wang Y, Pei J, et al. Super efficiency SBM-DEA and neural network for performance evaluation[J]. Information Processing & Management, 2021, 58(6): 102728.
[11]Li J, Li S, Cheng L, et al. BSAS: A Blockchain-Based Trustworthy and Privacy-Preserving Speed Advisory System[J]. IEEE Transactions on Vehicular Technology, 2022, 71(11): 11421-11430